Liquid Crystals
Publication details, including instructions for authors and subscription information:
http://www.informaworld.com/smpp/title~content=t713926090

Antiferroelectric behaviour of achiral mesogenic polymer mixtures

E. A. Soto Bustamante[a]; S. V. Yablonskii[b]; B. I. Ostrovskii[b]; L. A. Beresnev[a]; L. M. Blinov[b]; W. Haase[a]
[a] Institute of Physical Chemistry, THD, Darmstadt, Germany [b] Institute of Crystallography, RAS, Moscow

To cite this Article Bustamante, E. A. Soto , Yablonskii, S. V. , Ostrovskii, B. I. , Beresnev, L. A. , Blinov, L. M. and Haase, W.(1996) 'Antiferroelectric behaviour of achiral mesogenic polymer mixtures', Liquid Crystals, 21: 6, 829 — 839
To link to this Article: DOI: 10.1080/02678299608032899
URL: http://dx.doi.org/10.1080/02678299608032899

LIQUID CRYSTALS, 1996, VOL. 21, NO. 6, 829-839

Antiferroelectric behaviour of achiral mesogenic polymer mixtures

by E. A. SOTO BUSTAMANTE†, S. V. YABLONSKII‡, B. I. OSTROVSKII‡,
L. A. BERESNEV†, L. M. BLINOV*‡, and W. HAASE†

†Institute of Physical Chemistry, THD, Petersenstr.20, Darmstadt 64287, Germany
‡Institute of Crystallography, RAS, 117333, Leninsky pr.59, Moscow

(Received 11 March 1996; in final form 26 June 1996; accepted 17 July 1996)

X-ray structure determination and pyroelectric and piezoelectric measurements have been carried out on mesogenic mixtures composed of achiral side chain polymers and their monomers. Certain mixtures show antiferroelectric polarization hysteresis loops in the mesophase which was shown to be a bilayered smectic C, while the two components of the mixtures taken alone show no antiferroelectricity. The results obtained on the polymer–monomer mixtures are interpreted in terms of the smectic C structure with alternating tilt which, from a symmetry viewpoint, is allowed to be antiferroelectric. The antiferroelectric mixtures, on being cooled to the glassy state under a d.c. electric field applied, reveal high pyroelectric coefficients with prospects for application as IR detectors.

1. Introduction

Since the beginning of this century achiral (with mirror symmetry) crystalline ferro- and antiferro-electrics have been investigated very extensively [1]. As a rule, they manifest so-called *proper* ferroelectricity when the spontaneous polarization arises as a primary order parameter due to dipole–dipole interactions, although there are some examples of *improper* crystalline ferroelectrics where $\mathbf{P}_S$ is a secondary order parameter. Among proper ferroelectrics there have been found crystalline polymers such as polyvinylidene fluoride (PVDF) and its copolymers. Weak ferroelectric properties have also been observed in an achiral lamellar mesophase, that is in a non-crystalline material [2].

On the other hand, chiral tilted mesophases (C*, F*, I*, etc.), including those of polymers, manifest both ferroelectric [3, 4] and antiferroelectric [5, 6] properties. The mechanism of ferroelectricity in these systems is quite specific: a tilt of elongated chiral molecules, that is the order parameter of a tilted phase, results in a polar ordering of their short axes (and their transverse dipole moments) perpendicular to the tilt plane. The $\mathbf{P}_S$ vector lies in the plane of a smectic layer perpendicular to the tilt plane. Such materials also belong to the class of improper ferro- and antiferro-electrics.

A search for *achiral* analogues of *mesomorphic* ferro- and antiferro-electrics is still a challenge to researchers, both theoreticians and experimentalists. Prost and Barois [7] predicted a 'longitudinal' proper ferroelectric where the spontaneous polarization arose due to the dipole–dipole interaction, is directed along the normal to the smectic layers and is allowed even in the smectic A phase. Improper ferroelectric and antiferroelectric ordering may arise due to specific intermolecular interactions which favour parallel alignment of electric dipoles as was discussed in [8, 9]. In a tilted smectic phase of a non-chiral substance, the $\mathbf{P}_S$ vector must lie in the tilt plane. It might be at a certain angle to the layer planes [8] or lie in the layer plane, as was discussed theoretically by Brand, Cladis and Pleiner [10, 11]. Ferroelectric order has also been predicted for non-chiral discotic mesophases formed by bowl-like molecules [12].

Few recent experiments seem to be in accordance with such theoretical predictions. An achiral mesophase composed of so-called polyphilic compounds [8] manifests a rather small $\mathbf{P}_S$ value [2] of the order of $10\,\mathrm{nC\,cm^{-2}}$. Much higher $\mathbf{P}_S$ magnitudes, of the order of $100\,\mathrm{nC\,cm^{-2}}$ have been reported by Swager *et al.* at the Budapest International Liquid Crystal Conference [13] for discotic (bowl-like) mesogens. However, ferro- or antiferro-electric properties were never observed in achiral mesogenic polymers. Moreover, to our knowledge, there have been no reports on crystalline polymer antiferroelectrics (all copolymers of PVDF are ferroelectric). In our search for novel polar materials we have found, rather unexpectedly, an interesting system with very unusual properties [14]. Here we present the first example of antiferroelectric behaviour of mesogenic mixtures composed of an achiral side chain polymer and its monomer. Of particular interest is the fact that neither

---

*Author for correspondence.

of the two components alone manifests this behaviour. The mixtures show polarization hysteresis curves in the smectic C phase and, on being cooled to the glassy state under an applied d.c. electric field, reveal high pyroelectric responses of potential interest for application as IR detectors [15].

2. Materials and their characterization

Originally, an extremely unusual electric behaviour was observed for mixtures of an achiral side chain methacrylate polymer PM6R8 with its monomer M6R8, figure 1, and most of the results presented here are related to these mixtures. In addition, we have carried out studies on mixtures of shorter alkyl chain homologues of the original pair (PM6R6 and M6R6) and on the acrylate analogues of the same pair, PA6R8 and A6R8, respectively. All three pairs mentioned show the antiferroelectric behaviour. On the contrary, a polymer–monomer pair having no lateral hydroxy group, PM6B8 and M6B8, taken for comparison, was 'electrically inactive'. The chemical formulae of all the substances studied are shown in figure 1.

The preparation of the monomers was carried out by refluxing an ethanolic solution of the appropriate substituted aniline and aldehyde in the presence of a catalytic amount of hydroquinone (HQ) for 2 hours. After two recrystallizations from methanol, pale yellow plates of the monomer were obtained in 70% yield. The methacrylate polymers were synthesized by radical polymerization of the corresponding monomers in toluene, in a sealed vial degassed with nitrogen, for 72 hours at 60°C, using α,α'-bis-azoisobutyronitrile (AIBN) as initiator. Subsequent precipitations of the swollen polymers with methanol from concentrated toluene solutions gave the yellow products in 70–80% yield.

Measurements of the optical rotatory power were carried out using a Perkin-Elmer 241 polarimeter. No trace of optical activity was found in solutions of $4\,\mathrm{g\,l^{-1}}$ concentration of the polymers or monomers in tetrahydrofuran. The molecular weight, $\bar{M}_W$, and the polydispersity index, $\bar{M}_W/\bar{M}_n$ for each polymer was determined by gel permeation chromatography (GPC) (Waters 510 microflow pump, Waters IR 410 detector) using polymethyl methacrylate (PMMA) as standard (ultrastyragel columns, tetrahydrofuran as eluent and a flow rate of $1\,\mathrm{ml\,min^{-1}}$). The data on the molar mass distribution

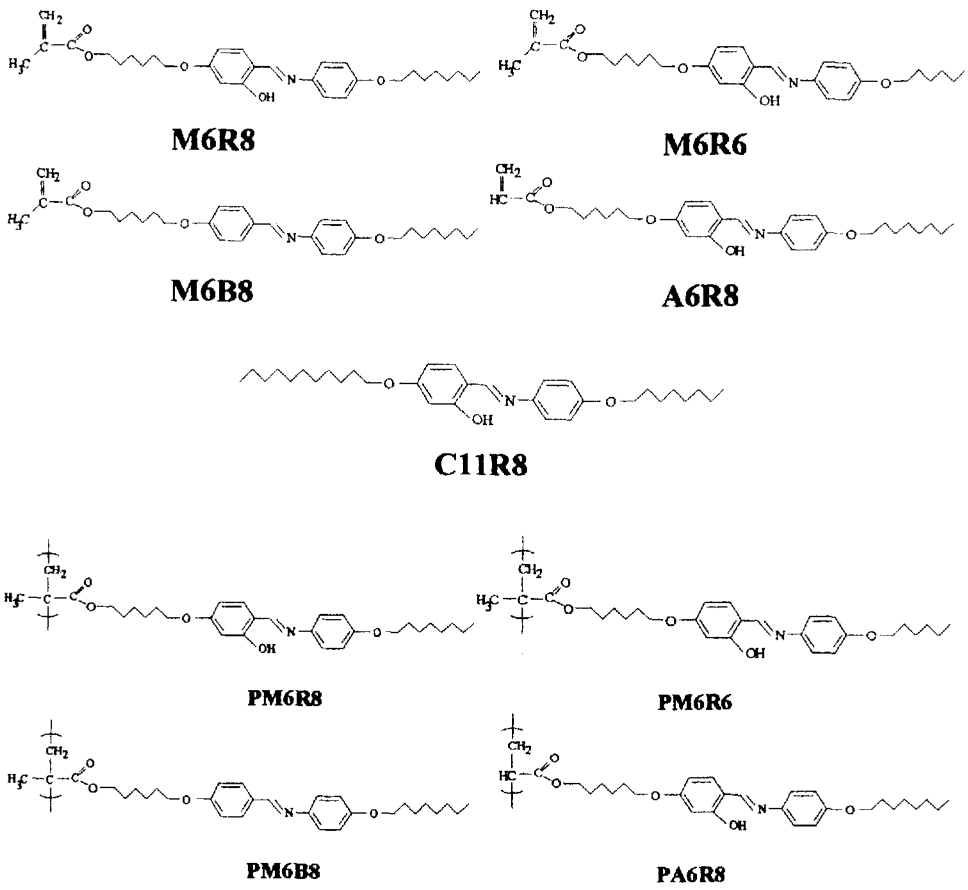

Figure 1. Chemical formulae of the monomers and polymers investigated, with their abbreviations.

Table 1. Phase transition temperatures (°C) and molecular weights for the polymers investigated.

Polymer	Phase behaviour	$\bar{M}_w$	$\bar{M}_w/\bar{M}_n$
PM6R8	g 93 S_c 184 I	81·500	2·1
PM6R6	g 82 S_c 157 S_A 173 I	54·300	2·4
PM6B8	g 80 S_c 161 I	64·500	1·9
PA6R8	g 60 S_c 180 I	85·200	5·8

Table 2. Phase transition tempertures (°C) and molecular lengths L (Å) for the monomers investigated.

Monomer	Transition tempertures	L
M6R8	Cr 54 S_A 96 I	34·0
M6R6	Cr 63 S_A 95 I	31·5
M6B8	Cr 71 S_A 114 I	34·0
A6R8	Cr 59 S_A 119 I	32·5
C11R8	Cr 60 S_A 119 I	35·2

for the polymers, as well as the transition temperatures determined by DSC and microscopic observations are summarized in table 1. The transition temperatures and molecular lengths (calculated with standard computer simulation software) of the corresponding monomers are given in table 2. A detailed description of the synthesis and characterization of intermediate and end products will be presented elsewhere [16].

In the most important cases (PM6R8, M6R8, their mixture in a 74:26 ratio and polymer PM6B8), X-ray structure determinations have been carried out. X-ray measurements were performed using a two-circle STOE diffractometer with a linear position-sensitive detector for data collection (CuK_α radiation) [17]. The longitudinal resolution was at the level $\Delta q_\parallel = 4 \times 10^{-3}\ \mathrm{A}^{-1}$ (full width at half maximum, FWHM). The components of the diffraction vector $q_\parallel$ and $q_\perp$ were parallel and perpendicular to the layer normal, respectively: $q = (4\pi/\lambda)\sin\theta$ (θ is scattering angle and λ is the wavelength of the radiation). Thus measurements of the longitudinal correlation length were limited by the value $\xi_\parallel = 2/\Delta q_\parallel \approx 500$ Å.

An X-ray study in the wide scattering angle region ($q_\perp \geqslant 1\ \mathrm{A}^{-1}$) provides data on the positional correlations in the plane of the smectic layers. These measurements were performed using flat-plate photographs and a KARD diffractometer with a two-coordinate detector [18, 9]. To derive the intensity contour maps from the two-dimensional images, the following procedure was used. First the number of radial cross-sections with an azimuthal step of 5° was recorded. The intensity distribution in each cross-section was divided into discrete groups from 1 to 4 (the maximum intensity was set equal to 4). In this way contours of equal intensity in gradations 1, 2 and 3 were displayed.

X-ray diffraction measurements were performed both on powder specimens (thin-wall glass capillaries) and on well oriented thin films. Oriented samples were prepared using the shear alignment technique. The polymer was placed between two glass plates and heated to the temperature of the mesophase, close to the transition into the isotropic liquid. Then, to provide a shear, the cover glass was repeatedly (and circularly) moved relative to the substrate. On fast cooling to room temperature, oriented textures with the smectic planes parallel to the film surface were maintained. The resulting films had thicknesses from 50 to 100 μm.

3. Electric measurements

To study the electric behaviour of our materials we used two techniques very sensitive to the incidence of any (spontaneously or field induced) polarized state, namely measurements of the pyroelectric and piezoelectric response. Cells consisted of two ITO covered, untreated glass plates with teflon spacers of thickness about 8 and 110 μm for pyroelectric and piezoelectric measurements, respectively. The cells were filled with materials in the isotropic phase either by capillary forces (for thin cells it takes about an hour) or by pressing the substance between the two electrodes. Cells were placed in a thermal jacket with optical windows.

For pyroelectric measurements, we used a pulse technique described in [19] in detail. A 100 μS pulse of a Nd^{3+} YAG laser was used to provide a small local temperature change ΔT in a sample. Laser radiation ($\lambda = 1{\cdot}06\ \mu\mathrm{m}$) was partly absorbed in the ITO layers. The pyroelectric response was measured as a pulse voltage across the load resistor $R_L = 100\ \mathrm{k}\Omega$ using a wide band amplifier and a storage oscilloscope. D.c. fields of various strengths were applied to the sample in order to measure hysteresis loops in pyroresponse-bias voltage coordinates. The data were recorded and processed with an IBM/PC computer.

The temperature dependence of the spontaneous polarization (on an arbitrary scale) was calculated by integrating the pyroelectric voltage, which is proportional to the pyroelectric coefficient γ, according to equation (1) (T_I is the transition temperature to the isotropic phase):

$$P_s(T) = \int_{T_I}^{T} \gamma(T)\,\mathrm{d}T \qquad (1)$$

Then the correct scale for γ and $\mathbf{P}_S$ was introduced by comparison of the pyroelectric response at a certain temperature with the value measured for a known ferroelectric substance [20] in a new cell made from the

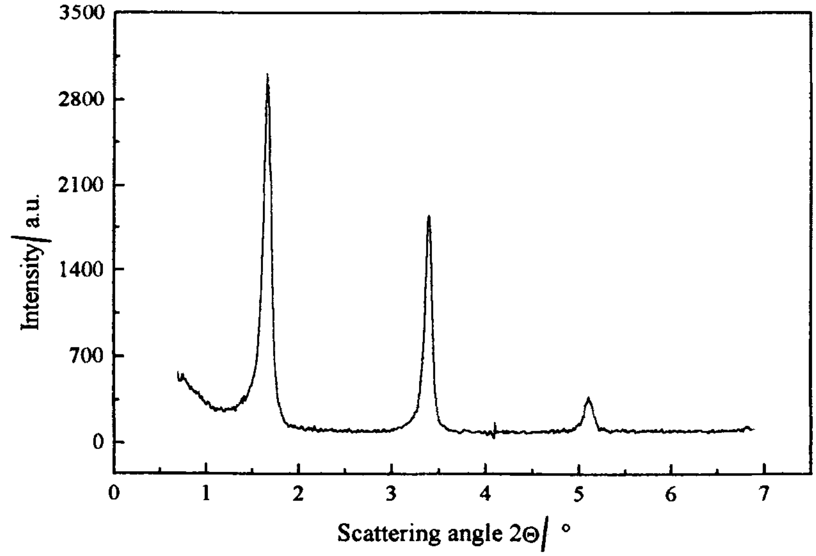

Figure 2. X-ray diffraction patterns in the small angle scattering region for a PM6R8-M6R8 (74:26) mixture; bilayer smectic C phase, $T = 120°C$. The second and third order reflections in the direction of the smectic layer normal $q_{\|}$ are very pronounced.

same ITO covered glasses (to have the same light absorption). A great advantage of the pyroelectric technique in comparison with conventional transient current or Sawyer–Tower hysteresis measurements is the ability to measure a static value of the polarization at virtually zero frequency. It may be applied to materials which switch slowly, such as, for example, chiral ferroelectric polymers with a high molecular mass [4].

The piezoelectric method has also been described earlier [21]. The substance is submitted to an oscillating pressure of 10^4 Pa provided by a loudspeaker at 86 Hz. The pressure is delivered by an acoustic $\lambda/4$-waveguide to one of the two opposite open edges of a cell. This perturbs the material and induces the piezoelectric voltage across the electrodes. A piezoelectric signal is detected at the frequency of the applied sound by a lock-in amplifier and plotted using an X-Y recorder. The signal is proportional to the total macroscopic polarization of the material and may be expressed [22] in terms of the piezoelectric modulus d_{31}. Advantages of this technique are simplicity and very high sensitivity to any macroscopic polarization of a cell; a disadvantage is the difficulty of calibration to obtain the absolute value of the polarization.

4. Experimental results

4.1. *X-ray data*

Originally, an anomalous electric behaviour was observed in a PM6R8-M6R8 (74:26) mixture within the range of existence of its smectic C phase. Thus, investigation of the structure of this phase seemed to be absolutely necessary.

The X-ray pattern of the compound below the isotropic transition exhibits sharp inner reflections and diffuse outer halos. The inner reflections are a set of 00*n* resolution limited peaks at $2\pi n/d$, where n is an integer ($n = 1$–3) and d is the layer spacing, figure 2. The diffuse outer peaks centred at $q_{\perp} \approx 1{\cdot}4\,\text{Å}^{-1}$, correspond to the average intermolecular distances 4·3–4·4 Å in the smectic planes, figure 3. These peaks are well fitted by the Lorentzian line shapes (dotted line). The corresponding in-plane correlation length $\xi_{\perp}$ is of the order of 6–10 Å; thus the molecular packing within a smectic layer may be considered as liquid-like.

It should be emphasised that in the mixtures under study (at least up to 33% concentration of monomers), X-ray diffraction revealed one set of 00*n* reflections only, which is characteristic of a uniform (ideal mixing) state.

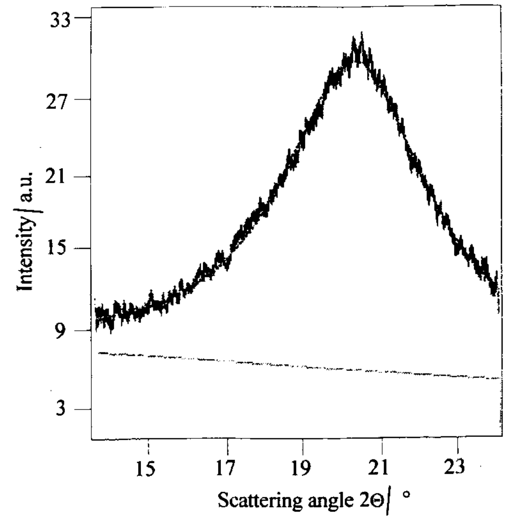

Figure 3. X-ray intensity profile in the large angle scattering region for a PM6R8-M6R8 (74:26) mixture; bilayer smectic C phase, $T = 120°C$.

X-ray measurements do not reveal broadening of 00*n* peaks or any additional diffuse scattering from admixed monomers. This means that the monomers randomly occupy the bilayers formed by the polymer matrix. No indication was found of any segregation of mixture components or phase separation.

With decreasing temperature, the layer spacing calculated from figure 2 varies with temperature in the range of 54–51 Å, being always much larger than the length of a mesogenic side chain ($L \approx 33$ Å). This implies some form of bilayer arrangement of the side groups in the smectic planes. We can assume a bilayer structure in which the side groups are tilted with respect to the normal to the layers. In another structural model, the side chains, being orthogonal to the smectic planes, might partly overlap each other (in an interdigitated structure). In order to make a choice between the two structural models, two-dimensional X-ray patterns from oriented films had to be analysed, see figure 4. It is clearly seen that the outer reflections are split into two intense spots lying to the right and left of the equator line ($q_\perp$ direction). This points to a tilt of the side groups with respect to the normal to the layers. The azimuthal angles of the intensity maxima for the spots with respect to the $q_\perp$ direction give an average value of the molecular tilt angle β. Note, that in orthogonal smectics, the outer reflections are always centred at the equator line. The tilt angle derived from the X-ray scattering, $\beta = 35$–$39°$, is in good agreement with the tilt angle calculated from the layer spacing data at low temperatures: $\beta = \arccos d/2L \approx 33$–$35°$.

Thus, according to the X-ray data, the PM6R8-M6R8 (74:26) mixture shows a phase transition from the isotropic into a bilayered smectic C phase. The X-ray studies were also carried out separately on pure polymer PM6R8 and its monomer M6R8. In the only mesophase found in the monomer, the smectic phase interlayer spacing $d \approx 35$ Å is very close to the molecular length $L \approx 33$ Å; thus, according to the X-ray and optical data, this phase should be referred to as smectic A. The polymer was shown to have the same bilayered smectic C phase as the (74:26) mixture. However high order reflections are more pronounced for the mixture (e.g. the ratio of the second to the first harmonic intensities for the mixture is twice as large as that for the pure polymer). In addition, in the pure polymer, the interlayer spacing monotonically decreases with temperature, consistent with an increase in the tilt angle. In the mixtures with the monomer, the interlayer distance is slightly larger and depends non-monotonically on temperature. The temperature behaviour of the interlayer distance has been measured for two mixtures, PM6R8-M6R8 (74:26) and (67:33) (the latter has even more pronounced antiferroelectric properties). For instance, in mixture (67:33), with decreasing temperature the interlayer distance changes non-monotonically: first, in the range 160–100°C it increases (from 53 to 55 Å), then in the range 100–25°C, it decreases (down to 51 Å in the glassy state). Both the more pronounced high order reflections and the anomalous increase in the spacing of the C phase close to the transition into the isotropic state point to a specific mutual packing of the monomer molecules and the side chain groups of the polymer that is strongly dependent on temperature.

Therefore, we conclude that both the pure polymer and its mixtures with the monomer have a bilayer struc-

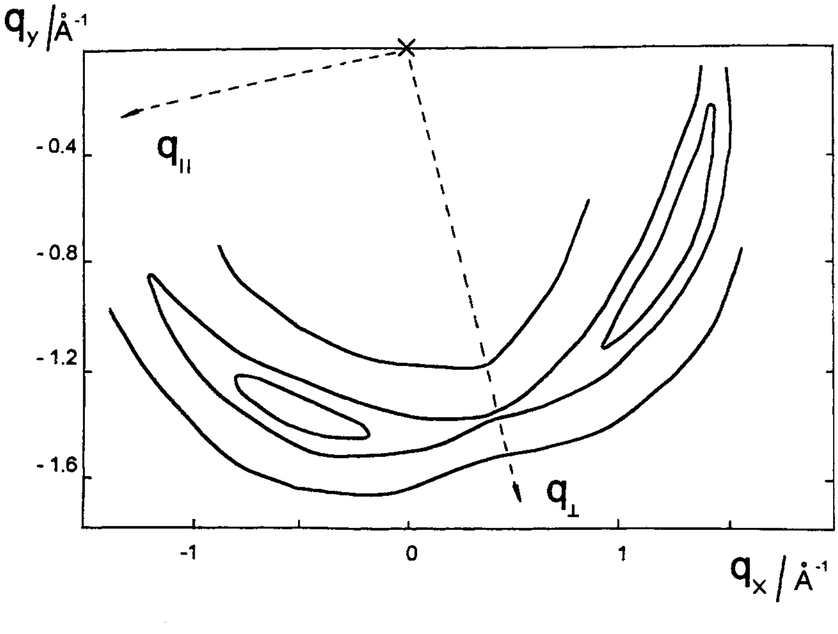

Figure 4. X-ray diffraction patterns in the wide angle scattering region for an oriented film of a PM6R8-M6R8 (75:25) mixture; frozen bilayer smectic C phase, $T = 20°$C. q_x and q_y are the coordinates of the two-dimensional detector; the components of the scattering wave vector $q_{\|}$ and $q_\perp$ lie along the layer normals and in the plane of the smectic layers, respectively. The small angle peaks shown in figure 2 are omitted because of the intensity scale difference.

ture in which the mesogenic side groups are tilted with respect to the layer normal of the smectic C phase. Four possible structures consistent with our X-ray data are sketched in figure 5. The first case (*a*) is a conventional smectic C, the second and third models correspond to a smectic C with regularly alternating directions of the tilt, with fractures of the structure (changes in tilt direction) taking place in the regions of either the tails (structure *b*) or the heads (structure *c*) of the mesogenic groups. Such alternating structures have earlier been reported for both polymer smectics C (main chain [23] and side chain [24]) and achiral low molecular weight mesogens [25]. In the fourth structure (*d*), a change of the molecular tilt occurs in both the tail and the head regions.

Note a remarkable difference between the (*b*) and (*c*) structures on the one hand and structure (*d*) on the other. Imagine that the dipole moment of a mesogenic group is directed from its head, attached to the main chain, to its free end and that the mesogenic groups are free to rotate around their longitudinal axes (liquid-like smectic layers). Then, considering projections of the dipoles on the smectic layer plane in cases (*b*) and (*c*), respectively, the in-plane polarization occurs only in the regions of either the tails or the heads, P_t or P_h. The possible directions of polarization are shown by arrows. In structure (*d*), both P_t and P_h are allowed. Both bilayered structures (*b*) and (*c*) are always antiferroelectric. The structure (*d*) is also *antiferroelectric* as long as $P_t = P_h$. If, however, free rotation is not assumed and the transverse components of dipole moments play a dominant role, the polarization might vanish in the regions of, say, the heads ($P_h = 0$) and a net macroscopic polarization P_t appears, so that structure (*d*) becomes *ferroelectric*, as was discussed in [10]. In a more general case of finite, but not equal magnitudes of P_t and P_h, structure (*d*) is *ferrielectric*.

4.2. *Pyro- and piezo-electric data for PM6R8-M6R8 mixtures*

Figure 6 shows the pyroelectric coefficient (*a*) and macroscopic polarization (*b*) as functions of temperature for mixtures of PM6R8 and M6R8 at various concentrations (in wt %) of the monomer. All the measurements were carried out on cooling 8–10 μm thick cells under d.c. bias field $E = 12\,\mathrm{V\,\mu m^{-1}}$. At zero field, no pyroelectric response is observed on cooling from the isotropic phase down to room temperature. With the bias field applied, the field induced pyroresponse (and polarization) in the isotropic phase ($T > 170°\mathrm{C}$) is still negligible for all of the mixtures. On transition at the clearing point (on cooling) to the bilayer smectic C phase, a sharp increase in the signal, in some cases by more than an order of magnitude, is easily seen in figure 6(*a*). The polarization permanently increases on cooling (figure 6(*b*)), although its growth is less pronounced in the glassy state.

The value of the macroscopic polarization both in the mesophase and in the glassy state has a well pronounced maximum as a function of monomer concentration, as displayed in figure 7. Neither the monomer nor pure

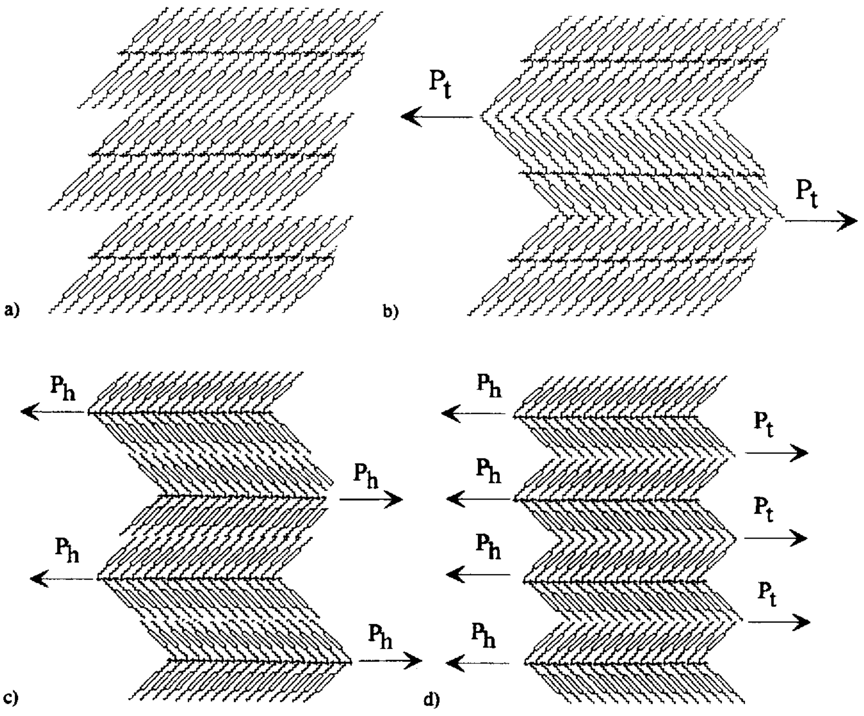

Figure 5. Four possible packings of the mesogenic groups of a side chain polymer in the bilayer smectic C phase: (*a*) uniform tilt; (*b*), (*c*) alternating tilt with in-plane antiferroelectric order; (*d*) alternating tilt with possible in-plane antiferro- ferro- or ferri-electric order. P_t and P_h are virtual polarizations in the regions of the tails and the heads of the mesogenic units.

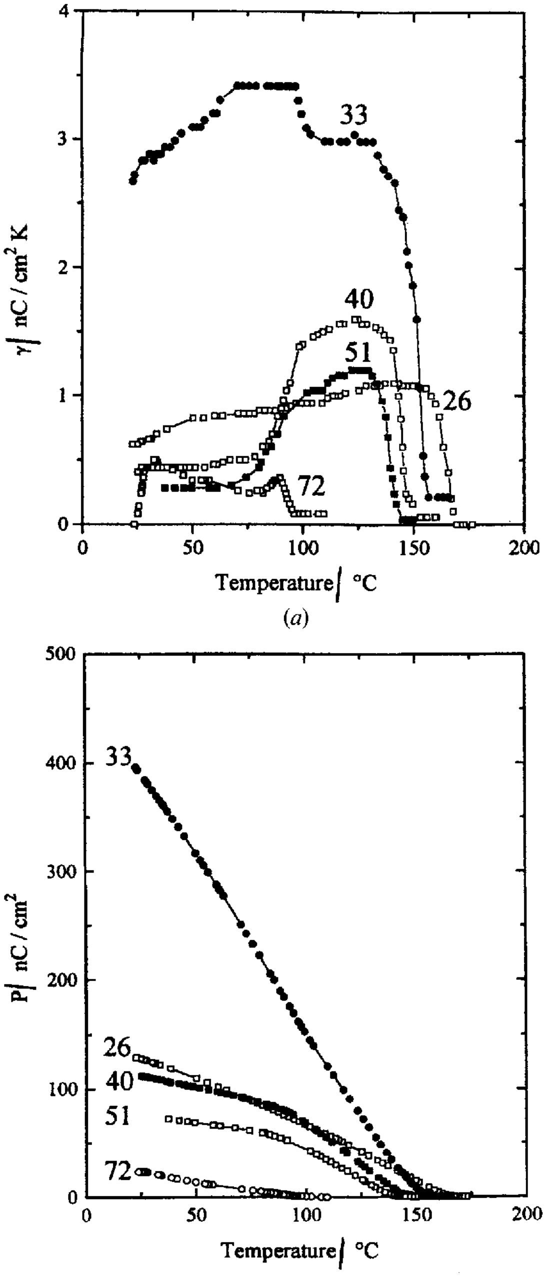

Figure 6. Temperature dependences of (*a*) the pyroelectric coefficient taken with negative sign for convenience of plotting and (*b*) the macroscopic polarization calculated by integration of the curves for the pyro-coefficients of mixtures of PM6R8 and M6R8 at various concentrations (in wt %) of the monomer. The temperature scans were made on cooling under a d.c. bias field, $E=12\,\mathrm{V\,\mu m^{-1}}$.

polymer shows a pyroelectric response, and the optimum response is achieved for a mixture with approximately 33% of the monomer.

The voltage dependence of the macroscopic polarization is extremely non-linear. At low voltages, the field induced polarization increases linearly with field and rapidly relaxes after field switching off. However, above a certain threshold the polarization grows in a super-linear way, and the field induced state has a certain memory (about half a minute). At these voltages, a double hysteresis loop expressed in coordinates of 'd.c. bias-pyroresponse' (instead of polarization, in conventional techniques) is easily measured, as shown in figure 8. Each of the consecutive points in the loops shown was taken half a minute after application of the corresponding voltage. Such loops are typical of antiferroelectrics; they correspond to three stable states, one with zero polarization (the field off state) and two with the spontaneous polarization oriented along two possible directions of the external field. The essential difference of our system from solid and liquid crystalline (chiral) antiferroelectrics is the rather slow response. It should be mentioned that no electro-optical response has been observed under either a.c. or d.c. voltage.

Strong field non-linearity was confirmed by measurements of the piezoelectric response of a PM6R8-M6R8 (74:26) mixture (figure 9(*a*)). As has been shown in detail [22], the piezoelectric coefficient in a glassy state can be calculated from the experimentally available piezoelectric voltage U by the following simple formula:

$$d_{31}=\frac{UC}{4LR\Delta p} \qquad (2)$$

where C is the capacity of the cell and cables, R is the radius of the polymer disk-shaped sample, Δp is the pressure difference and L is the penetration length of the deformation, dependent on the thickness of the sample h and Poisson ratio σ. Figure 9(*b*) shows the temperature dependences of piezoelectric coefficient d_{31} measured on heating a sample which was previously poled on cooling with various applied d.c. bias voltages. For calculation we used the following numbers: $C=30\,\mathrm{pF}$, $R=1\,\mathrm{mm}$, $\Delta p=10^4\,\mathrm{Pa}$, $\sigma=0{\cdot}34$, $h=110\,\mu\mathrm{m}$, $L=0{\cdot}65\,h$. The steep growth of the resulting piezoresponse is observed at slightly lower field strength (about $4\,\mathrm{V\,\mu m^{-1}}$) than that in the case of the pyroelectric measurements on $10\,\mu\mathrm{m}$ thick cells (figure 8).

In the glassy state, the pyroelectric response remains stable for a long time. Some samples stored at room temperature retained their polarization for almost a year. The best magnitude of the pyro-coefficient in the glassy state, $\gamma=2{\cdot}4\,\mathrm{nC\,cm^{-2}\,K}$ measured for a PM6R8-M6R8 mixture with 33% of the monomer is comparable with that observed for strongly poled PVDF films [1] and is at least one order of magnitude higher than the value typical of chiral polymer $\mathrm{S_C^*}$ ferroelectrics in their glassy state. On heating with no field applied, the material looses its memory. This is seen in figure 10,

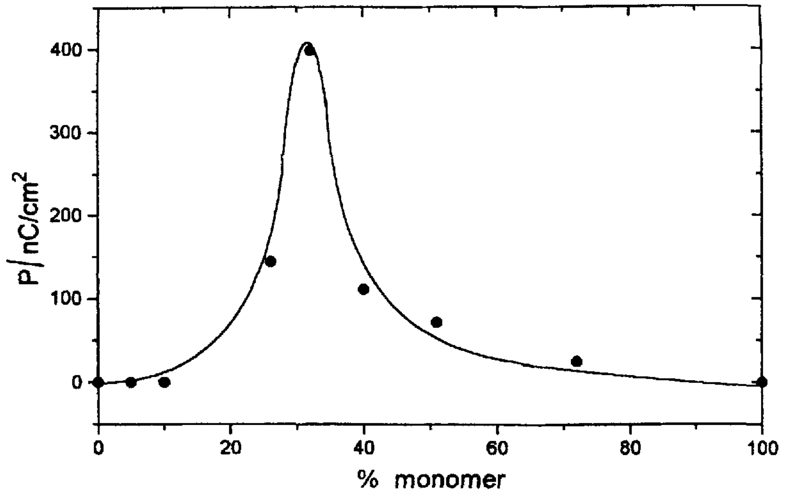

Figure 7. Maximum values of the macroscopic polarization (taken at room temperature after cooling to the glassy state) for mixtures of PM6R8 and M6R8 versus concentration of the monomer. The line is a guide for the eye.

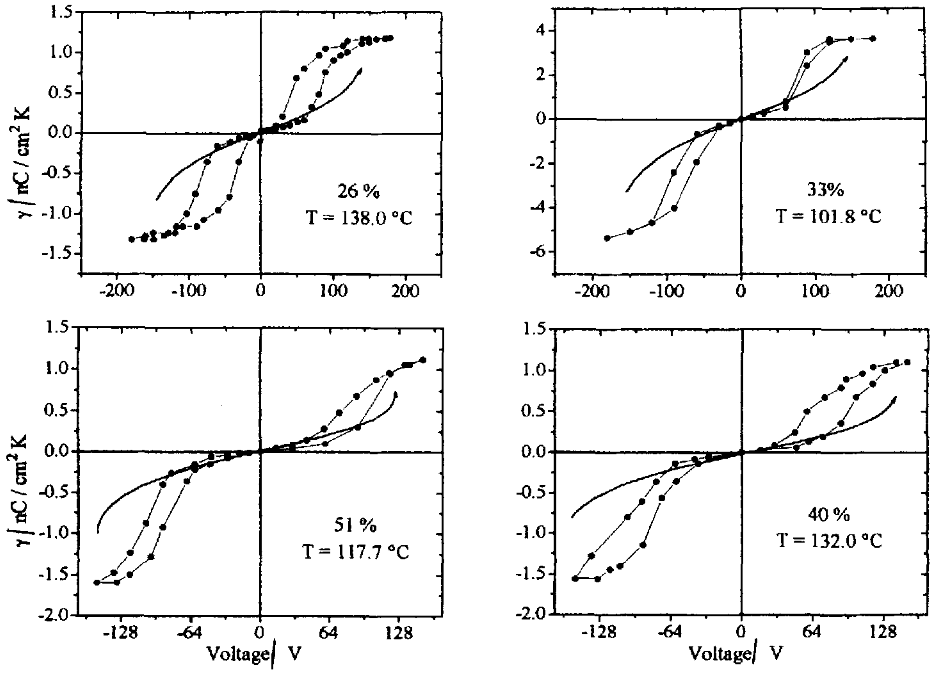

Figure 8. Quasi-static antiferroelectric loops expressed in coordinates of d.c. bias voltage-pyroelectric coefficient obtained for mixtures PM6R8 and M6R8 at different concentrations of the monomer. All curves are measured at different temperatures corresponding to the maximum values of the pyroelectric coefficients.

where temperature dependences of the pyro-coefficient (which has been induced by a field on cooling scans, figure 6 (*a*)) are shown for the heating scans. The memory is lost in the mesophase essentially before the transition into the isotropic liquid, except for the most viscous 26% mixture. This loss is consistent with the existence of three stable states in the antiferroelectric mesophase, one of which (the field off state) corresponds to zero polarization.

4.3. *Other materials*

The pyroelectric measurements were also performed for the other materials shown in figure 1. Two new polymer-monomer pairs with the same (33 wt %) concentration of the corresponding monomer, namely, PM6R6-M6R6 (67 : 33) and PA6R8-A6R8 (67 : 33) manifest similar antiferroelectric properties to those discussed above. This may be illustrated by figure 11, where the temperature dependences of the pyroelectric coefficients (taken on cooling under a d.c. bias electric field of 12 V μm) are shown. The magnitude of the macroscopic polarization reached in the glassy state is 130 and 310 nC cm^{-2} for PM6R6-M6R6 and PA6R8-A6R8, respectively. In the mesophase range, an antiferroelectric loop similar to those shown in figure 8 has been measured for the PM6R6-M6R6 pair.

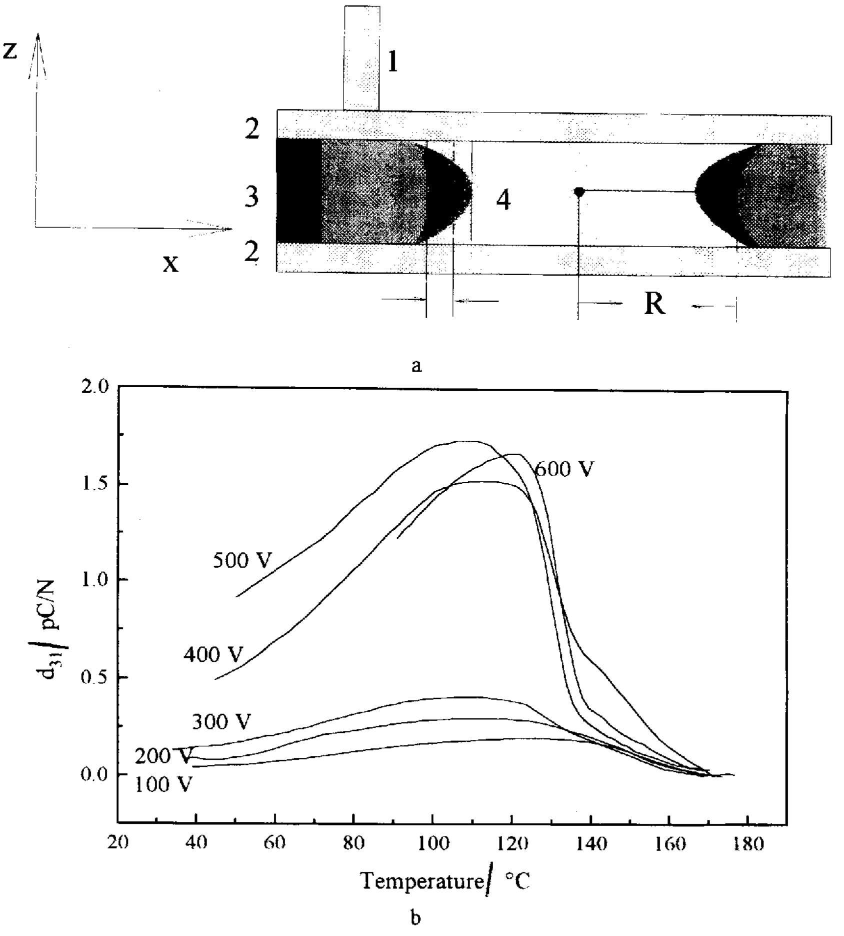

Figure 9(*a*). Geometry of the piezoelectric experiment: (1) acoustic pipe to apply pressure in the X-direction; (2) glasses covered with conductive layers to detect the piezo-voltage in the Z-direction; (3) teflon spacer; (4) polymer sample. (*b*). Temperature dependences of the piezoelectric coefficient d_{31} measured on heating a sample which had previously been poled on cooling with various applied d.c bias voltages; PM6R8-M6R8 (74:26) mixture; cell thickness = 110 μm.

On the other hand, antiferroelectric properties have not been observed for the other materials studied. It was already mentioned that not one of the polymers or monomers taken alone was electrically active. Some of the polymer–monomer pairs taken at the same (33 wt %) concentration of monomer, such as PM6R8-C11R8, PM6B8-M6B8, PM6R8-M6B8 and PM6B8-M6R8, were also electrically inactive. We will discuss this situation below.

5. Discussion

Our experimental results on achiral PM6R8-M6R8 mixtures are consistent with either of the two antiferroelectric structures shown in figures 5 (*b*) and 5 (*c*). Indeed X-ray data on the mesophase unambiguously show the typical bilayered smectic C structure which is allowed to be polar only in the case when polarization lies in the tilt plane. However, the pure polymer PM6R8 also has a smectic C structure, but is electrically inactive. It is reasonable to assume that the pure polymer has the conventional structure, shown in figure 5 (*a*). Therefore, a role of the monomer additive is to induce one of the smectic structures with alternating tilt. This role of the monomer additives in generating new structures has been reported before [26].

In the field off state, the macroscopic polarization in the mesophase is zero. With increasing field, the bilayers with in-plane polarization opposite to the field reorient in the field direction and a macroscopic polarization appears. Two field directions result in two quasi-stable states and a double loop typical of antiferroelectrics. The maximum magnitude of the macroscopic polarization measured ($400\,\mathrm{nC\,cm^{-2}}$) may be accounted for if we assume that all the mesogenic units of both polymer and monomer (with molecular weight about 500) have dipole moment projections on the field direction of about 1 D, which is quite reasonable. On transition to the glassy state, the field induced macroscopic polarization becomes frozen in and the material manifests a pyroelectric response comparable with that of typical, proper polymer ferroelectrics. At the moment we cannot make a choice between the structures shown in figures 5 (*b*) and 5 (*c*); both are consistent with our data.

It is much more difficult to understand the molecular mechanism of the phenomenon. Let us note first that antiferroelectricity is observed only in the case when

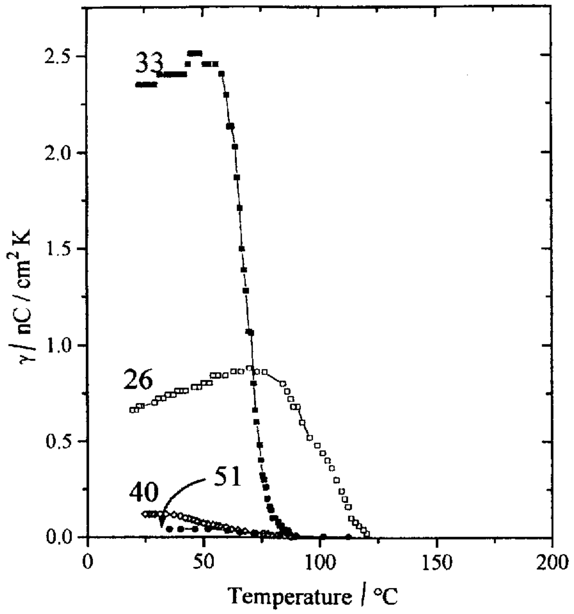

Figure 10. Temperature dependences of the pyroelectric coefficient for PM6R8-M6R8 mixtures with various concentrations of the monomer. The measurements were made on heating without a d.c. bias field, after the poling process shown in figure 6 had been terminated in the glassy state.

both components of a polymer–monomer pair have a hydroxy group, no matter whether we are dealing with an acrylate or a methacrylate main chain or with eight or six carbon atoms in the alkyloxy end tail. The absence of the hydroxy group in at least one of the components of a mixture eliminates antiferroelectricity. In our opinion the hydroxy group may play a double role. On the one hand, it may be conducive to the in-layer polar packing due to dipole–dipole interaction well known from the physics of crystalline ferroelectrics [1]. On the other hand, as soon as the antiferroelectric structure with in-plane polarization is established, for some other reasons, the hydroxy group may also provide a component of the dipole moment necessary for high polarization.

What is strange is that a non-polymerizable ligand C11R8, having a hydroxy group exactly in the same position as in monomer M6R8, was mixed with polymer PM6R8 but did not induce antiferroelectricity in the mixture. One possible reason is that the molecular structure of this additive is too symmetric and is incompatible with the side chain polymer. Thus a structure with alternating twist cannot form.

On the other hand, we cannot completely exclude the possibility of a virtual polymerization which might occur in the applied electric field when a monomer has an unsaturated chemical bond. Indeed, after application of a strong electric field to PM6R8-M6R8 mixtures, we observed a noticeable shift of the clearing point to higher temperatures. Perhaps, the field induced polymerization itself is conducive to the appearance of polar order. It should be mentioned, however, that antiferroelectric properties in the mesophase are reproduced well after several cycles of cooling and heating the cells with a strong electric field applied to the electrodes. Thus, in our opinion, field induced polymerization cannot be the main reason for antiferroelectric behaviour.

6. Conclusion

In conclusion, the first example of antiferroelectric behaviour of mesogenic mixtures composed of achiral side chain polymers and their monomers is presented. The mixtures show polarization hysteresis curves in the mesophase (but not in the isotropic phase) measured by the pyroelectric technique. This behaviour was also confirmed by the piezoelectric measurements. Of particular interest is the fact that none of the two components alone manifests this behaviour. By X-ray analysis the mesophase was shown to be a bilayered smectic C, with

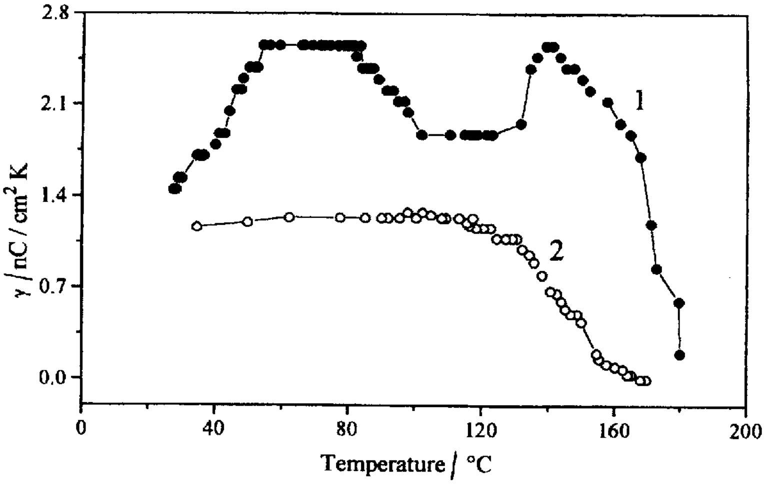

Figure 11. Temperature dependences of the pyroelectric coefficient for mixture PM6R6-M6R6 (67 : 33), curve 1, and for mixture PA6R8-A6R8 (67 : 33), curve 2, on cooling down under a d.c. bias electric field of 12 V μm^{-1}.

liquid-like layers. The results are interpreted in terms of a smectic C structure with alternating tilt which, from the symmetry viewpoint, is allowed to be an antiferroelectric. The monomer additive is assumed to be generating the alternating tilt structure in the side chain polymer. The macroscopic polarization measured in the mesophase reaches values of about 300 nC cm^{-2} which require a dipole moment projection onto the smectic plane of about 1 D per mesogenic unit. The mixtures, on being cooled to the glassy state under a d.c. applied electric field, reveal high pyroelectric coefficients comparable to those observed in proper polymer ferroelectrics and raising prospects for application in radiation detectors [15].

We are grateful to Prof. S. A. Pikin for stimulating discussions, Dr. S. Palto and Dr. Th. Weyrauch for supplying the software for the pyroelectric measurements, Dr. Yu. Galyametdinov for the synthesis of some intermediate products and Dr. Disselhof of Deutsche Kunststoff Institute for polymer molar mass determination. The financial support from Deutsche Telekom is acknowledged. We also acknowledge DFG support (AZ 4381/113/112/01) for bilateral Russian-German cooperation, VW support (AZ I/70668) for co-operation with East Europe, and INTAS Foundation support (grants 94-1482 and 95-IN-RU-128).

References

[1] Lines, M. E., and Glass, A. M., 1977, *Principles and Applications of Ferroelectrics and Related Materials*, (Oxford: Clarendon Press).

[2] Tournilhac, F., Blinov, L. M., Simon, J., and Yablonsky, S. V., 1992, *Nature*, **359**, 61.

[3] Meyer, R. B., Liebert, L., Strzelecki, L., and Keller, P., 1975, *J. Phys. France, Lett.*, **36**, L69.

[4] Shibaev, V. P., Kozlovsky, M. V., Beresnev, L. A., Blinov, L. M., and Plate, N. A., 1984, *Polym. Bull.*, **12**, 299.

[5] Beresnev, L. A., Blinov, L. M., Baikalov, V. A., Pozhidayev, E. P., Purvanetskas, G. V., and Pavlyuchenko, A. I., 1982, *Mol. Cryst. liq. Cryst.*, **89**, 327.

[6] Hiji, N., Chandani, A. D. L., Nishiyama, S., Ouchi, Y., Takezoe, H., and Fukuda, A., 1988, *Ferroelectrics*, **85**, 99.

[7] Prost, J., and Barois, P., 1983, *J. Chim. Phys.*, **80**, 65.

[8] Tournilhac, F., Bosio, L., Nicoud, J.-F., and Simon, J., 1988, *Chem. Phys. Lett.*, **145**, 452.

[9] Blinov, L. M., Lobko, T. A., Ostrovskii, B. I., Sulianov, S. N., and Tournilhac, F., 1993, *J. Phys. II France*, **3**, 1121.

[10] Brand, H. R., Cladis, P., and Pleiner, H., 1992, *Macromolecules*, **25**, 7223.

[11] Cladis, P., and Brand, H. R., 1993, *Liq. Cryst.*, **14**, 1327.

[12] (*a*)Lin, L. (Lam, L.), 1982, *Wuli(Beijin)* **11**, 171; (*b*) 1987, *Mol. Cryst. liq. Cryst.*, **146**, 41.

[13] Swager, T. M., Serrette, A. G., Knawby, D. M., and Zheng, H., 1994, *15 Int. Liq. Cryst. Conf.*, Budapest, Abstract Vol. 2, p. 771.

[14] Soto Bustamante, E. A., Yablonskii, S. V., Beresnev, L. A., Blinov, L. M., Ostrovskii, B. I., and Haase, W., 1996, 61st Bunsen-Kolloquium on Ferroelectric Organic Materials in Thin Films, February 1996, Darmstadt, Abstract p. 44.

[15] Soto Bustamante, E. A., Yablonskii, S. V., Beresnev, L. A., Blinov, L. M., Haase, W., Dultz, W., and Galyametdinov, Yu. G., 1995, German Patent Application 195 47 934.3.

[16] Ostrovskii, B. I., Soto Bustamante, E. A., Galyametdinov, Yu. G., Yablonskii, S. V., and Haase, W., *Mol. Mat.* (to be published).

[17] Haase, W., Fan, Z. X., and Muller, H. J., 1988, *J. chem. Phys.*, **89**, 3317.

[18] Andrianova, M. E., Kheiker, D. M., and Popov, A. N., 1982, *J. appl. Cryst.*, **15**, 626.

[19] Beresnev, L. A., and Blinov, L. M., 1981, *Ferroelectrics*, **33**, 129.

[20] Blinov, L. M., 1994, *Modern Topics in Physics*, edited by A. Buka, (Singapore: World Scientific), p. 337.

[21] Blinov, L. M., Baikalov, V. A., Barnik, M. I., Beresnev, L. A., Pozhidayev, E. P., and Yablonsky, S. V., 1987, *Liq. Cryst.*, **2**, 121.

[22] Yablonsky, S. V., Kats, E. I., Kozlovsky, M. V., Weyrauch, T., Soto Bustamante, E. A., Subachius, D. B., and Haase, W., 1994, *Mol. Mat.*, **3**, 318.

[23] Watanabe, J., and Hayashi, M., 1989, *Macromolecules*, **22**, 4088.

[24] Mensinger, H., Biswas, A., and Poths, H., 1992, *Macromolecules*, **22**, 3156.

[25] Nishiyama, I., and Goodby, J. W., 1992, *J. Mater. Chem.*, **2**, 1015.

[26] Leube, H., and Finkelmann, H., 1991, *Makromol. Chem.*, **192**, 1317.